nature genetics

Genome-wide functional analysis of pathogenicity genes in the rice blast fungus

Junhyun Jeon[1], Sook-Young Park[1,5], Myoung-Hwan Chi[1], Jaehyuk Choi[1], Jongsun Park[1], Hee-Sool Rho[1], Soonok Kim[1], Jaeduk Goh[1], Sungyong Yoo[1], Jinhee Choi[1], Ju-Young Park[1], Mihwa Yi[1], Seonyoung Yang[1], Min-Jung Kwon[1], Seong-Sook Han[2], Byeong Ryun Kim[2], Chang Hyun Khang[3], Bongsoo Park[1,5], Se-Eun Lim[1], Kyongyong Jung[1], Sunghyung Kong[1], Maruthachalam Karunakaran[1], Hong-Sik Oh[1], Hyojeong Kim[1], Seryun Kim[1], Jaejin Park[1], Soyoung Kang[1], Woo-Bong Choi[4], Seogchan Kang[3] & Yong-Hwan Lee[1]

Rapid translation of genome sequences into meaningful biological information hinges on the integration of multiple experimental and informatics methods into a cohesive platform. Despite the explosion in the number of genome sequences available[1], such a platform does not exist for filamentous fungi. Here we present the development and application of a functional genomics and informatics platform for a model plant pathogenic fungus, *Magnaporthe oryzae*[2]. In total, we produced 21,070 mutants through large-scale insertional mutagenesis using *Agrobacterium tumefaciens*–mediated transformation[3]. We used a high-throughput phenotype screening pipeline to detect disruption of seven phenotypes encompassing the fungal life cycle and identified the mutated gene and the nature of mutation for each mutant. Comparative analysis of phenotypes and genotypes of the mutants uncovered 202 new pathogenicity loci. Our findings demonstrate the effectiveness of our platform and provide new insights on the molecular basis of fungal pathogenesis. Our approach promises comprehensive functional genomics in filamentous fungi and beyond.

Decoding the plethora of available genome sequence information requires not only a diverse array of experimental and informatics tools but also systematic approaches for the seamless integration of such tools with the resulting data. Genome-wide high-throughput genetic screens have been conducted in several major model organisms using homologous recombination[4,5], insertional mutagenesis[6,7] and RNA interference[8–10]. Several gene manipulation tools exist for filamentous fungi, but a comprehensive platform for large-scale, systematic genetic screens to decipher gene function is still lacking, despite the importance and utility of such a system.

Many fungal species greatly affect human welfare by destroying crop plants[11] or by causing life-threatening diseases in immunocompromised individuals[12]. However, our understanding of the molecular mechanisms involved in host–pathogen interactions is limited to only a few aspects of infection and colonization. A comprehensive understanding of pathogenic mechanisms based on genomic sequences demands advanced genomics tools and infrastructures. A rapidly increasing list of recently sequenced fungal genomes provides tremendous opportunities for studying the biology and evolution underlying the pathogenic lifestyle. Here, we describe the development and application of a new functional genomics platform using the model plant pathogenic fungus *Magnaporthe oryzae*.

M. oryzae is a filamentous heterothallic ascomycete that causes rice blast disease. The fungus is an important model organism for investigating fungal infection–related development and pathogenicity owing to its genetic tractability[11]. Unlike most plant–fungal pathogen systems, the genomic sequences of both the fungus[13] and rice[14,15] are available, providing a unique opportunity to study a host–parasite interaction from both sides using functional genomic approaches. We carried out large-scale insertional mutagenesis of the *M. oryzae* strain KJ201 via *Agrobacterium tumefaciens*–mediated transformation (ATMT) and obtained 21,070 hygromycin-resistant mutants, which we tagged with transfer DNA (T-DNA). The T-DNA insertions showed mitotic and meiotic stability, and over 80% of the mutants were estimated to have a single copy of the T-DNA integrated into the genome. Assuming a genome size of ~38 Mb, an average gene length of ~1.7 kb[13] and random T-DNA insertion events, our mutant library was large enough to saturate ~61% of the genome[16].

To facilitate a rapid and comprehensive functional analysis of the mutants, we developed a high-throughput screening (HTS) system (**Fig. 1a**). We designed the HTS system to rapidly catalog the phenotypes and genotypes of the individual mutants, along with the

[1]Department of Agricultural Biotechnology, Center for Fungal Genetic Resources, and Center for Agricultural Biomaterials, Seoul National University, Seoul 151-921, Korea. [2]National Institute of Crop Science, Rural Development Administration, Suwon 441-857, Korea. [3]Department of Plant Pathology, The Pennsylvania State University, University Park, Pennsylvania 16802, USA. [4]Department of Biotechnology and Bioengineering, Dongeui University, Busan 614-714, Korea. [5]Current address: Department of Plant Pathology, The Pennsylvania State University, University Park, Pennsylvania 16802, USA. Correspondence should be addressed to Y.-H.L. (yonglee@snu.ac.kr).

Received 25 October 2006; accepted 8 February 2007; published online 11 March 2007; doi:10.1038/ng2002

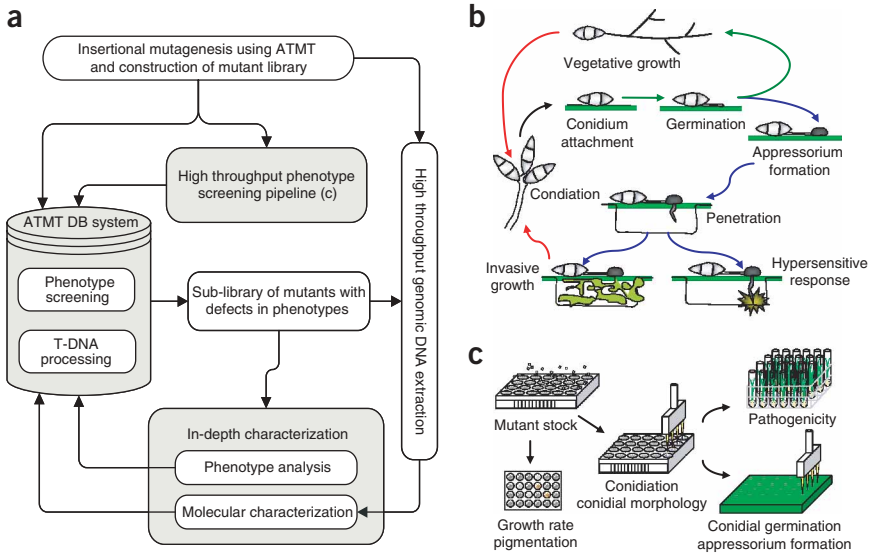

Figure 1 Schematic diagram of the high-throughput screening system and the life cycle of *Magnaporthe oryzae*. (**a**) ATMT was used to construct a library of insertion mutants. Each mutant was given an identification number based on its coordinates within a 24-well plate. During screening, the phenotypes of the individual mutants were assigned using a numeric scale. Data from the HTS were entered into the ATMT database system. We selected mutants with phenotypes of interest for in-depth phenotypic analysis and identified the T-DNA insertion sites. The resulting data were added to the ATMT database system. Genomic DNA for molecular characterization was extracted using our high-throughput DNA extraction protocol. (**b**) Asexual spores (conidia) are produced in the conidiophore. Once released, conidia germinate and follow one of two developmental fates depending on environmental cues. They develop a specialized infection structure, called the appressorium, and infect host plants, or they shift to a vegetative stage. Either way, conidia are produced to reinitiate the cycle. Checkpoints for vegetative growth, asexual reproduction and infection are indicated by green, red and blue lines, respectively. (**c**) Mutants were grown in 24-well plates and their growth rates and pigmentation were measured after 3 d and 6 d, respectively. Conidial suspensions were prepared from 6-d-old cultures, and the degrees of conidiation, conidial germination, appressorium formation and conidial morphology were subsequently examined on a green mirror under a light microscope. The remaining conidial suspensions were sprayed onto rice seedlings to assay their pathogenicities.

subsequently identified gene functions, using a relational database. During the screen, every stage of mutant processing and analysis was performed in a 24-well plate format, which greatly diminished the time and labor needed to label and handle the individual mutants.

Assigning phenotypes to mutants is one of the key steps in elucidating gene functions. Phenotypes manifested by genome, however, are so numerous and diverse that the detection of mutant phenotypes depends on the developmental stages examined and the assay conditions used. To address this issue, we used high-throughput phenotype screening (HPS) to assay alterations in seven traits (**Fig. 1b**,**c**) encompassing the entire life cycle of the fungus (**Fig. 1c** and **Supplementary Methods** online). Using HPS, we processed the entire library of 21,070 mutants as a primary screen. Next, we carried out an additional round of screening to confirm the phenotypes of the putative mutants selected during the primary screen. In combination, these screens yielded more than 180,000 data points—the most comprehensive phenotypic data set ever built for a filamentous fungus. In particular, we explored fungal pathogenicity extensively on a genomic scale using our miniaturized pathogenicity assay protocol (**Supplementary Methods**), which enabled us to circumvent the time and space constraints of typical large-scale inoculation assays (for example, 3–4 weeks of rice cultivation and a large greenhouse facility). Considering the emerging theme of conserved genes and functionalities between plant and animal pathogens[17], our interaction phenome data could provide new insights into the mechanisms involved in human and animal mycoses.

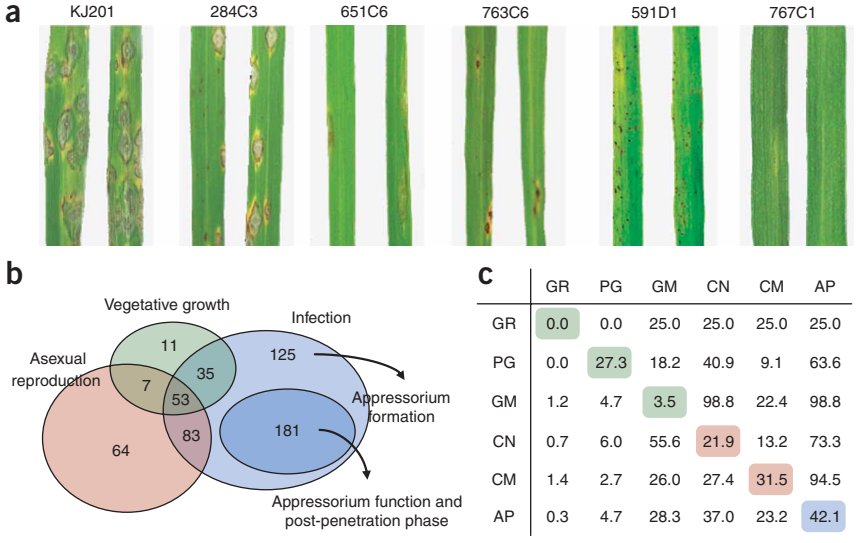

c

	GR	PG	GM	CN	CM	AP
GR	0.0	0.0	25.0	25.0	25.0	25.0
PG	0.0	27.3	18.2	40.9	9.1	63.6
GM	1.2	4.7	3.5	98.8	22.4	98.8
CN	0.7	6.0	55.6	21.9	13.2	73.3
CM	1.4	2.7	26.0	27.4	31.5	94.5
AP	0.3	4.7	28.3	37.0	23.2	42.1

Figure 2 Composition and pairing analysis of phenotypes among pathogenicity-defective mutants. (**a**) The pathogenicity-defective mutants showed a wide spectrum of pathogenicity. The wild-type strain KJ201 developed typical spindle-shaped lesions that often coalesced, whereas the mutants showed reduced numbers of lesions that sometimes failed to proliferate, small specks or no signs of infection. (**b**) A Venn diagram showing the number of mutants with defects in vegetative growth (growth rate, pigmentation and conidial germination), asexual reproduction (conidiation and conidial morphology) and infection (appressorium formation, penetration, and invasive growth). (**c**) Pairing analysis of the mutant phenotypes, showing the percentage of mutants with a combination of defects (as a ratio of column to row). The ratio of mutants with defects in only one trait is shaded in colors corresponding to the colors used in **b**. GR, growth rate; PG, pigmentation; CN, conidiation; GM, conidial germination; AP, appressorium formation; CM, conidial morphology.

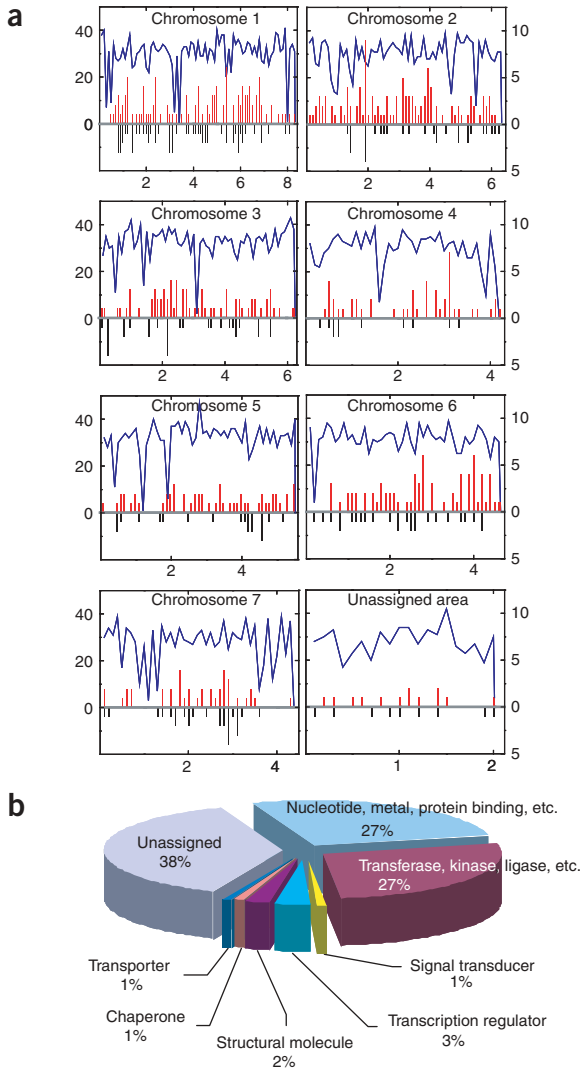

Figure 3 Distribution of T-DNA insertions over the chromosomes and functional categorization of the T-DNA–tagged genes. (**a**) Distribution of T-DNA insertions over the chromosomes. The genome was divided into windows of 100 kb. The numbers of T-DNA insertions in each window are plotted as bars perpendicular to the chromosomes (represented by horizontal gray lines). Red bars indicate the insertion frequency in each gene (where a gene is defined as the sequence ranging from 1,000 bp upstream to 500 bp downstream of the ORF), and black bars represent the insertion frequency in the intergenic regions. The blue lines represent the best-fitting function for the gene distribution. 'Unassigned area' indicates the collection of genomic contigs that cannot be mapped onto chromosomes. The *x* axis of each graph indicates the length of each chromosome in Mb. The left and right *y* axes indicate the number of genes and T-DNA insertions, respectively. (**b**) Gene ontology (GO) categorization of genes tagged by the T-DNA. The percentage of hits to GO categories with a 'molecular function' annotation is indicated.

From the pathogenicity-driven mutant screen, we selected 559 putative pathogenicity-defective mutants for further characterization (**Fig. 2a** and **Supplementary Table 1** online). We examined the remaining six traits in these mutants. This analysis showed that most of the mutants were defective in infection, asexual reproduction or both (**Fig. 2b**). Among the six phenotypes, growth rate and pigmentation showed limited association with pathogenicity, but defects in appressorium formation and conidiation were strongly correlated with defects in pathogenicity, providing genome-scale support for the importance of these two developmental stages in pathogenicity. Furthermore, many mutants had defects in multiple phenotypes (**Fig. 2c**). Except for growth rate and pigmentation, each trait showed various degrees of association with the other traits, suggesting the involvement of common genes in multiple cellular processes. However, a considerable number of mutants (32.4%) had defects only in pathogenicity (**Fig. 2b**). These mutants may be defective in appressorium functionality before cuticle penetration or during the post-penetration phase when the fungus suppresses plant defenses and establishes invasive growth.

To complement the HPS system, we performed in-depth phenotypic assays on selected mutants to quantify the altered phenotypes. In parallel with the phenotype screening, characterization of the nature of the mutations in isolated mutants was carried out using a high-throughput genomic DNA extraction protocol (see Methods), thermal asymmetric interlaced (TAIL) PCR[18] and sequencing. We verified the accuracy of TAIL-PCR in identifying the T-DNA insertion sites in the mutants by inverse PCR. After we determined the sequences flanking a given T-DNA, our database automatically located the T-DNA insertion site within the fungal genome. Using TAIL-PCR, we identified a total of 741 T-DNA–tagged locations (TTLs) from the mutants to date (**Supplementary Tables 2** and **3** online). In most cases (~72%), the flanking sequences of right border were amplified. We characterized both ends of T-DNA insertion in 41 mutants, indicating that the mutation is the result of insertion rather than translocation. Although many of the TTLs were in pathogenicity-defective mutants, analysis of the TTLs showed that the T-DNA insertions were relatively evenly distributed throughout all of the chromosomes (**Fig. 3a**). Furthermore, we found little correlation between the T-DNA insertion frequency and gene density.

In-depth phenotypic and genotypic analysis of pathogenicity-defective mutants uncovered 203 independent loci involved in pathogenicity, creating the largest unbiased set of putative pathogenicity genes for a single species (**Supplementary Table 4** online). T-DNA insertions in these loci reduced or abolished the ability of the fungus to cause disease, resulting in a reduced number and/or size of lesions or no visible symptoms. Our inventory of pathogenicity genes included one previously known gene, *NTH1* (ref. 19), encoding neutral trehalase, and genes putatively involved in the MAP kinase pathway or carnitine metabolism, both of which have been shown to be required for pathogenicity[20,21] in *M. oryzae*. Searching PHI-base (see URLs section of Methods) for possible orthologs (maximum *e* value cutoff: 1×10^{-10}) of pathogenicity genes from other plant pathogens uncovered an additional 11 matches (~6.9%), supporting the robustness of our HTS system (data not shown). Most of the ORFs identified, however, had little or no homology with genes whose functions are known. Gene ontology (GO) analysis showed diverse predicted functions, such as signal transducer, structural molecule, transporter and transcriptional regulator, with no preferential enrichment in any category in comparison with the analysis of all genes in *M. oryzae* (**Fig. 3b**). These results suggest a genetic basis for fungal pathogenicity, which requires complex coordination of cellular processes and mobilization of many cellular components and structures. Targeted disruption of the ORFs (see Methods) for 15 pathogenicity-defective mutants confirmed the linkage between the T-DNA insertions and the observed phenotypes in 14 mutants (**Supplementary Table 5** online).

Abnormalities in the pathogenicity-defective mutants included, but were not limited to, aberrant conidial morphology (**Fig. 4a**), failure to produce appressoria (**Fig. 4b**) and the inability to penetrate

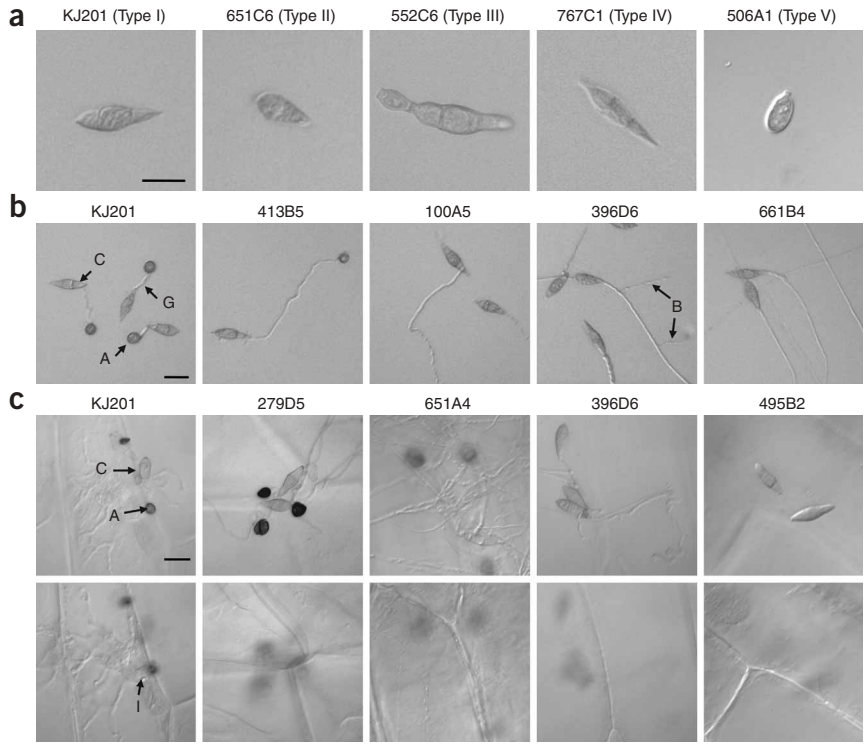

Figure 4 Representative phenotypes of the mutants. (**a**) Five types of conidial morphology shown by KJ201 and its mutants. KJ201 shows typical conidia (Type I); 651C6, short conidia (Type II); 552C6, deformed conidia (Type III); 767C1, elongated conidia (Type IV) and 506A1, short conidia lacking septa (Type V). (**b**) Response of the germ tube to a hydrophobic surface. KJ201 shows normal appressorium formation; 413B5, delay in appressorium formation; 100A5, long, meandering germ tube; 396D6, branching germ tube and 661B4, long germ tube. (**c**) Penetration into onion epidermal cells. The upper panel indicates the surface of the plant cells, and the lower panel shows the inside of the plant cells. KJ201 shows penetration and invasive growth; 279D5 and 651A4, inability to penetrate; 396D6, failure to form appressoria and 495B2, lack of germination. A, appressorium; B, branch; C, conidium; G, germ tube; I, invasive hyphae.

the plant cuticle layer (**Fig. 4c**). Mutants defective in asexual development showed multifarious conidial lengths, numbers of cells and morphologies (**Fig. 4a**). In these mutants, some T-DNA insertions occurred in ORFs homologous with *RAC* from *Colletotrichum trifolii* (552C6: MGG_02731)[22] and *ERD2* from *Saccharomyces cerevisiae*[23] (659D4: MGG_02423). The conidial morphology shown by the 552C6 mutant was especially noteworthy because its length and shape showed a marked contrast to that of KJ201 (**Fig. 4a**, Type III). In addition, conidia of the 552C6 mutant did not produce appressoria, implying a wide-ranging role for the putative GTPase in the development of *M. oryzae*. The roles of yeast *ERD2* in protein transport and secretion through the Golgi network[23] suggest the importance of these cellular processes in the asexual and pathogenic development of filamentous fungi. Among the mutants defective in appressorium formation, the degree of defect ranged from a complete inability to form appressoria to the production of a significantly reduced number of appressoria (**Fig. 4b**). We also identified several ORFs in those mutants with known homologs. For example, disruption of MGG_05343 (661B4) and MGG_00883 (413B5), homologs of *amyR* from *Aspergillus nidulans*[24] and *BCK1* from *S. cerevisiae*[25], respectively, blocked or delayed appressorium formation. The *amyR* gene encodes a transcription factor that regulates the production of enzymes for carbon use, and *BCK1* encodes a MAP kinase kinase kinase regulating cell wall integrity. It remains to be determined whether both genes retain their roles in *M. oryzae* as regulators of carbon use and cell wall integrity, but our analysis showed that the ORFs are required for appressorium formation on hydrophobic surfaces. As *M. oryzae* evolved to become a successful plant pathogen, the function of these genes, which are shared by a group of fungal species, may have changed in order to aid in establishing infection-specific morphogenesis.

Our web-based ATMT database (see URLs section of Methods) houses all of the data from HPS, in-depth screening and TTLs, connecting over 180,000 data points. The system links the phenotypes of the mutants to the genes tagged by T-DNA in an interactive way so that database users can infer the functions of affected genes. The phenotypic data can be searched and retrieved selectively from the system based on user-defined criteria, which consequently guides the selection of mutants with specific phenotypes. Although many databases have been built for tracking and storing biological data[26,27], our database is unique and versatile in that it is capable of relating and analyzing heterogeneous data sets in multiple contexts.

Our functional genomics and informatics platform provides a model that demonstrates how technologies can be integrated to uncover gene functions on a genomic scale. Further studies of the candidate pathogenicity genes identified in this work will allow breakthroughs in our understanding of the mechanisms and evolution underlying fungal pathogenicity, as only a handful of pathogenicity genes are known in fungi[17]. We anticipate that our model approach will be applied to other fungi, thus contributing to the speed and feasibility with which functional genomic analysis of microbial eukaryotes are achieved. Finally, our mutant library will be an invaluable resource through the distribution of mutants and easy access to our phenotypic and genotypic data.

METHODS

Fungal strain, culture conditions and insertional mutagenesis. *M. oryzae* strain KJ201, obtained from the National Institute of Crop Science (Korea), was used as the wild-type strain throughout this work. Fungal cultures were grown on V8 agar medium in 24-well plates at 25 °C under continuous fluorescent light. *Agrobacterium tumefaciens* strain AGL-1 harboring the pBHt2 vector[28] was used for transforming KJ201 as previously described[3].

Mutant library construction. For single-spore isolation, spores from 12 mutants were spread onto the surface of 2% water agar in a Petri plate (50 mm in diameter) that was partitioned into 12 fan-shaped sections. We obtained single conidial isolates by picking germinating conidia under a light microscope at 40× to 100× magnification and transferring them onto fresh 24-well plates containing V8 agar medium. For long-term storage, all isolates were transferred into additional 24-well plates (two replicates) and dried with finely hashed filter paper after being cultured for 5 d at 25 °C under constant fluorescent light. To prevent cross-contamination, the 24-well plates containing the desiccated mutants were sealed with a tape sheet (Qiagen). The mutants were stored at –70 °C in the

24-well format in a plastic box that holds 40 plates at the Center for Fungal Genetic Resources (Seoul National University).

High-throughput DNA extraction. Extraction of genomic DNA was performed as previously described[29] using a 24-prong plastic grinder customized to fit 24-well plates.

TAIL-PCR and sequencing. TAIL PCR was carried out as previously described[18] with modifications. Instead of performing the tertiary PCR, the process was terminated after the secondary PCR, and any remaining primers and nucleotides were removed from the reaction mixture. The purified reaction mixture was then sequenced directly with a specific primer designed for tertiary PCR. Sequencing analysis was carried out using an ABI 3700 DNA sequencer (Applied Biosystems) following the manufacturer's instructions at the National Instrumentation Center for Environmental Management (Seoul National University).

Targeted disruption of loci tagged by T-DNA. Gene disruption was performed using two different PCR-based approaches. For targeted gene disruption, T-DNA (~2 kb) and both the 5′ and 3′ flanking regions (~1 kb on each side) were amplified from the mutant genomic DNA using a locus-specific primer pair to yield a DNA fragment of ~4 kb. The resulting PCR product was purified (LaboPass PCR; Cosmogenetech) and used to transform fungal protoplasts (5×10^7/ml) prepared from strain KJ201.

For the loci that were not suitable for this approach owing to the insertion of tandem arrays of T-DNA, targeted gene deletion was carried out using the modified double-joint PCR (DJ-PCR) method[30]. Both the 5′ and 3′ flanking regions of the T-DNA insertion site were amplified and fused to a 1.9-kb *hygB* cassette by PCR. Fungal protoplasts were transformed with the DJ-PCR product following purification.

Construction of the ATMT database system. The ATMT database was constructed using freely available software. A MySQL relational database server was used for storage and efficient retrieval of data from the high-throughput screening database and external databases, such as the *M. oryzae* genome database. An Apache web server was used to build the user interface and to connect the databases, in combination with PHP. The web-based input and output user interfaces were designed to accommodate the 24-well plate format used for the HTS. Perl, a widely used bioinformatics language, was used to automatically detect the T-DNA insertion site in the ATMT mutants, and a graphical representation and interface were implemented using PHP and GD (graphic library).

URLs. PHI-base can be found at http://www.phi-base.org/. The ATMT database can be accessed at http://atmt.snu.ac.kr. Analysis of the T-DNA insertion sites was performed using the *M. oryzae* genome database (release 5) (http://www.broad.mit.edu/), which consists of the genomic sequences and InterPro annotation (InterPro v. 12.0) (http://www.ebi.ac.uk/interpro/) and GO annotation databases (http://www.geneontology.org/).

Note: Supplementary information is available on the Nature Genetics website.

ACKNOWLEDGMENTS

We are grateful to K. Lee and N.J. Talbot for their comments and suggestions on the manuscript. This research was partially supported by a grant from the Biogreen21 project funded by the Rural Development Administration, by grants from the Crop Functional Genomics Center (CG1421) and the Microbial Genomics and Applications Center (0462-20060021) of the 21st Century Frontier Research Program funded by the Ministry of Science and Technology, and by Korean Research Foundation Grant (KRF-2004-005-F00013) to Y.H.L. Requests for materials should be addressed to Y.H.L. (yonglee@snu.ac.kr).

AUTHOR CONTRIBUTIONS

S.-Y.P., M.-H.C., J.J., H.-S.R., S.K., J.G. and S.Y. generated the mutants and performed high-throughput phenotype screening. J.C., J.-Y.P., M.Y., S.Y., S.-E.L. and M.-J.K. assisted in phenotype assessment. J.P., K.J., S.K., S.K., J.P., B.P. and S.K. developed the ATMT database. J.J., M.-H.C., S.Y., J.G., M.K. and W.-B.C. performed targeted knockout of the selected ORFs. S.-S.H. and B.R.K. performed pathogenicity tests on pot-grown rice plants. J.C., J.J., J.G., S.Y. and M.-H.C. performed TAIL PCR and sequence analysis. J.J., C.H.K., H.-S.O., H.K., S.K., S.K. and Y.-H.L. contributed to the writing of this paper. Y.-H.L. designed and directed this study.

COMPETING INTERESTS STATEMENT

The authors declare no competing financial interests.

Published online at http://www.nature.com/naturegenetics
Reprints and permissions information is available online at http://npg.nature.com/reprintsandpermissions

1. Galagan, J.E., Henn, M.R., Ma, L.J., Cuomo, C.A. & Birren, B. Genomics of the fungal kingdom: insights into eukaryotic biology. *Genome Res.* **15**, 1620–1631 (2005).
2. Couch, B.C. & Kohn, L.M. A multilocus gene genealogy concordant with host preference indicates segregation of new species, *Magnaporthe oryzae* from *M. grisea*. *Mycologia* **94**, 683–693 (2002).
3. Rho, H.S., Kang, S. & Lee, Y.H. *Agrobacterium tumefaciens*-mediated transformation of the plant pathogenic fungus, *Magnaporthe grisea*. *Mol. Cells* **12**, 407–411 (2001).
4. Giaever, G. *et al.* Functional profiling of the *Saccharomyces cerevisiae* genome. *Nature* **418**, 387–391 (2002).
5. Winzeler, E.A. *et al.* Functional characterization of the *S. cerevisiae* genome by gene deletion and parallel analysis. *Science* **285**, 901–906 (1999).
6. Bevan, M. & Walsh, S. The *Arabidopsis* genome: a foundation for plant research. *Genome Res.* **15**, 1632–1642 (2005).
7. Hirochika, H. *et al.* Rice mutant resources for gene discovery. *Plant Mol. Biol.* **54**, 325–334 (2004).
8. Andres, A.J. Flying through the genome: a comprehensive study of functional genomics using RNAi in *Drosophila*. *Trends Endocrinol. Metab.* **15**, 243–247 (2004).
9. Ashrafi, K. *et al.* Genome-wide RNAi analysis of *Caenorhabditis elegans* fat regulatory genes. *Nature* **421**, 268–272 (2003).
10. Berns, K. *et al.* A large-scale RNAi screen in human cells identifies new components of the p53 pathway. *Nature* **428**, 431–437 (2004).
11. Talbot, N.J. On the trail of a cereal killer: Exploring the biology of *Magnaporthe grisea*. *Annu. Rev. Microbiol.* **57**, 177–202 (2003).
12. Kwon-Chung, K.J. & Bennett, J.E. *Medical Mycology* (Lea and Febiger, Philadelphia, 1992).
13. Dean, R.A. *et al.* The genome sequence of the rice blast fungus *Magnaporthe grisea*. *Nature* **434**, 980–986 (2005).
14. Yu, J. *et al.* A draft sequence of the rice genome (*Oryza sativa* L. ssp. indica). *Science* **296**, 79–92 (2002).
15. Goff, S.A. *et al.* A draft sequence of the rice genome (*Oryza sativa* L. ssp. japonica). *Science* **296**, 92–100 (2002).
16. Krysan, P.J., Young, J.C. & Sussman, M.R. T-DNA as an insertional mutagen in *Arabidopsis*. *Plant Cell* **11**, 2283–2290 (1999).
17. Idnurm, A. & Howlett, B.J. Pathogenicity genes of phytopathogenic fungi. *Mol. Plant Pathol.* **2**, 241–255 (2001).
18. Liu, Y.G. & Whittier, R.F. Thermal asymmetric interlaced PCR: automatable amplification and sequencing of insert end fragments from P1 and YAC clones for chromosome walking. *Genomics* **25**, 674–681 (1995).
19. Foster, A.J., Jenkinson, J.M. & Talbot, N.J. Trehalose synthesis and metabolism are required at different stages of plant infection by *Magnaporthe grisea*. *EMBO J.* **22**, 225–235 (2003).
20. Xu, J.R., Staiger, C.J. & Hamer, J.E. Inactivation of the mitogen-activated protein kinase Mps1 from the rice blast fungus prevents penetration of host cells but allows activation of plant defense responses. *Proc. Natl. Acad. Sci. USA* **95**, 12713–12718 (1998).
21. Bhambra, G.K., Wang, Z.Y., Soanes, D.M., Wakley, G.E. & Talbot, N.J. Peroxisomal carnitine acetyl transferase is required for elaboration of penetration hyphae during plant infection by *Magnaporthe grisea*. *Mol. Microbiol.* **61**, 46–60 (2006).
22. Chen, C. & Dickman, M.B. Dominant active Rac and dominant negative Rac revert the dominant active Ras phenotype in *Colletotrichum trifolii* by distinct signalling pathways. *Mol. Microbiol.* **51**, 1493–1507 (2004).
23. Semenza, J.C., Hardwick, K.G., Dean, N. & Pelham, H.R. *ERD2*, a yeast gene required for the receptor-mediated retrieval of luminal ER proteins from the secretory pathway. *Cell* **61**, 1349–1357 (1990).
24. Tani, S. *et al.* Characterization of the *amyR* gene encoding a transcriptional activator for the amylase genes in *Aspergillus nidulans*. *Curr. Genet.* **39**, 10–15 (2001).
25. Lee, K.S. & Levin, D.E. Dominant mutations in a gene encoding a putative protein kinase (*BCK1*) bypass the requirement for a *Saccharomyces cerevisiae* protein kinase C homolog. *Mol. Cell. Biol.* **12**, 172–182 (1992).
26. Donofrio, N. *et al.* 'PACLIMS': a component LIM system for high-throughput functional genomic analysis. *BMC Bioinformatics* 10.1186/1471–2105–6-94 (2005).
27. Baker, E.J., Galloway, L., Jackson, B., Schmoyer, D. & Snoddy, J. MuTrack: a genome analysis system for large-scale mutagenesis in the mouse. *BMC Bioinformatics* 10.1186/1471–2105–5-11 (2004).
28. Mullins, E.D. & Kang, S. Transformation: a tool for studying fungal pathogens of plants. *Cell. Mol. Life Sci.* **58**, 2043–2052 (2001).
29. Rogers, S.O. & Bendich, A.J. Extraction of DNA from milligram amount of fresh, herbarium, and mummified plant tissue. *Plant Mol. Biol.* **5**, 69–76 (1985).
30. Yu, J.H. *et al.* Double-joint PCR: a PCR-based molecular tool for gene manipulations in filamentous fungi. *Fungal Genet. Biol.* **41**, 973–981 (2004).